Extended Abstracts of the 2019 International Conference on Solid State Devices and Materials, Nagoya, 2019, pp185-186

Band Alignment in Charge-Transfer-Type p^+-WSe_2/MoS_2 Tunnel FET

K. Nakamura[1], N. Nagamura[2], K. Ueno[3], T. Taniguchi[2], K. Watanabe[2], and K. Nagashio[1]

[1] The University of Tokyo, 7-3-1 Hongo, Bunkyo-ku, Tokyo 113-8656, Japan
[2] National Institute of Materials Science, 1-1 Namiki, Tukuba, Ibaraki 305-0044, Japan
[3] Saitama University, 255 Shimo Okubo, Sakura-ku, Saitama 338-8570, Japan
E-mail: nakamura@ncd.t.u-tokyo.ac.jp

Abstract: The type-III band alignment was observed only for 3 layer (L) MoS_2 in 1-5L MoS_2/p^+-WSe_2. Through this study, it is revealed that band alignment of p^+-WSe_2/MoS_2 TFET is controlled by the two different physical origins, that is, E_F modulation in WSe_2 by V_{TG} and electron transfer from MoS_2. Since both origins depend on the MoS_2 channel thickness, the band alignment is quite sensitive to the MoS_2 thickness.

1. Introduction

Tunnel field effect transistors (TFETs) are promising for the low power switching FETs which can overcome the theoretical limitation of the subthreshold swing (*S.S.* = 60 meV/dec) for conventional MOSFETs [1]. 2D-materials are expected to be suitable for TFETs because 2D-TFETs have short tunnel distance defined by van der Waals heterointerface, thereby gaining higher on-current than that for conventional 3D-TFETs. Although the p^+/n heterostructure is necessary to achieve the low *S.S.*, doping technique is still under development for both interstitially and chemically. Recently, we have found that p^+-WSe_2 doped chemically by WO_x can be stabilized in air by transferring it on *h*-BN, and observed band-to-band tunneling (BTBT) current in the p^+-WSe_2/4-layer (L) MoS_2 heterostructure [2]. However, its band alignment could not be changed from type II to type III even by applying the sufficient gate bias, although type-III band alignment is necessary to gain large BTBT current. In this study, p^+-WSe_2/MoS_2 heterostructures consisting of 1 - 5L MoS_2 were fabricated and their transport properties were investigated in order to reveal the MoS_2 thickness dependence on the band alignment of charge-transfer-type p^+/n heterostructure and achieve type-III band alignment.

2. Device fabrication

p^+-WSe_2 needs to be stable in air for the source of TFET. After forming WSe_2/WO_x by O_3 annealing at 200 °C for 1 h, WO_x side is transferred onto *h*-BN and p^+-WSe_2 is stabilized. After that, MoS_2 with suitable thickness (1 - 5L) is chosen by its contrast on PDMS and the p^+-WSe_2/MoS_2 heterostructures were fabricated via dry transfer method using PDMS under the alignment system. Ni/Au was deposited as source/drain electrodes after the electrode pattern formation by an electron beam lithography. Then, Y_2O_3 buffer layer (~1.5 nm), ALD-Al_2O_3 oxide layer (~30 nm) and Al top-gate electrode were formed. **Figure 1** shows (a) schematic illustration and (b) optical image of the top-gate p^+-WSe_2/2L-MoS_2 TFET device.

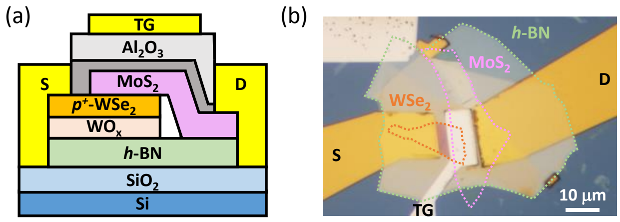

Fig. 1 (a) Schematic illustration and (b) optical image of the p^+-WSe_2/2L-MoS_2 TFET device.

3. Characterization of p^+-WSe_2/3L-MoS_2 TFET

Firstly, the p^+-WSe_2/3L-MoS_2 device with 30-nm-Al_2O_3 was fabricated. This device consists of thinner MoS_2 and Al_2O_3 than those in the previous p^+-WSe_2/4L-MoS_2 device with 60-nm-Al_2O_3 showing the type-II band alignment [2]. **Figure 2** shows the diode properties of 3L-MoS_2 device with various top gate voltage (V_{TG}) at 20 K. The current at reverse bias is due to BTBT because minority carriers have been suppressed at sufficiently low temperature. When V_{TG} is -9 ~ 15 V, BTBT current can flow at reverse bias and negative differential resistance (NDR) trend is clearly observed as the intersection of BTBT current and diffusion current at forward bias. The appearance of NDR trend indicates that type-III band alignment is achieved.

Figure 3(a) compares I_{DS}-V_{TG} at V_{SD} = -2 V (reverse bias) between the 3L-MoS_2 and previous 4L-MoS_2 devices. Higher on-current can be obtained in the 3L-MoS_2 device than that in the 4L-MoS_2 device mainly owing to type-III band alignment. *S.S.* of the 3L-MoS_2 device does not depend on the temperature and is increased by increasing I_{DS},

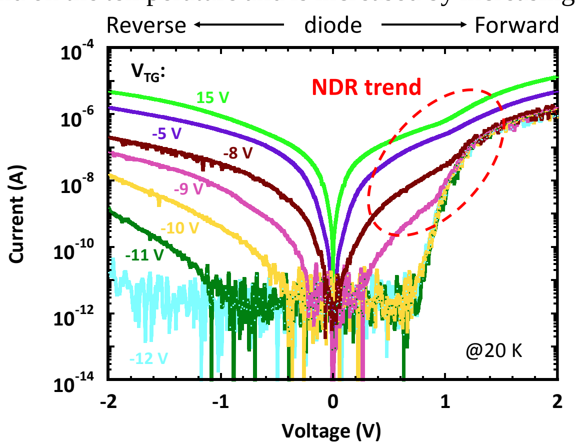

Fig. 2 Diode properties of p^+-WSe_2/3L-MoS_2 TFET at 20 K.

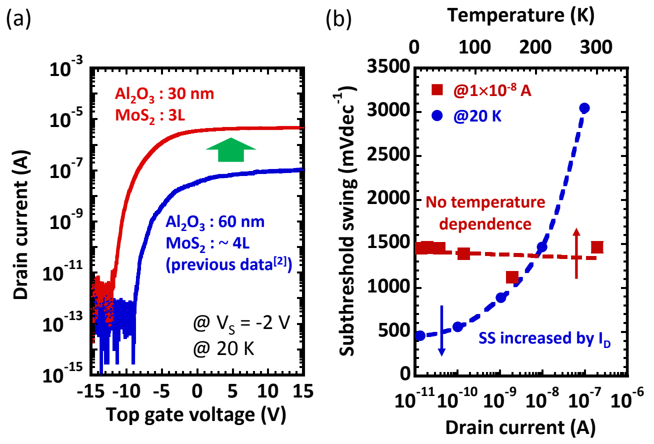

Fig. 3 (a) I_{DS}-V_{TG} curves of 3L- and 4L-MoS_2 devices. (b) *S.S.* as functions of I_{DS} and temperature.

as shown **Fig. 3(b)**. These characteristics also support that the current at reverse bias is indeed due to BTBT and p^+-WSe_2/3L-MoS_2 device is operated as TFET.

4. MoS_2 thickness effect to the band alignment

In order to reveal the relationship between MoS_2 thickness and the band alignment in p^+-WSe_2/MoS_2 device, **Figure 4(a)** compares diode properties of p^+-WSe_2/1-5L MoS_2 devices at V_{TG} = 15 V and 20 K. The 3L-MoS_2 device is only the type-III, while the other devices are the type-II because 1, 2 and 4L MoS_2 devices show BTBT current only at large reverse bias and the 5L-MoS_2 device does not show BTBT current even for reverse bias of -2 V. The brown arrows in **Fig. 4(a)** are defined as BTBT onset voltage (V_{BTBT}), which implies band offset between the conduction band minimum (CBM) for MoS_2 and the valance band maximum (VBM) for p^+-WSe_2. So V_{BTBT} can be modulated by V_{TG} and ideally reaches 0 V when band alignment is changed from type II to type III for the 3L-MoS_2 device, as shown in **Fig. 4(b)**. However, V_{BTBT} saturates before reaching 0 V for the other devices, although it is evident that Fermi level (E_F) in MoS_2 is sufficiently modulated for all the thickness cases. This suggests that the restriction to type II results from p^+-WSe_2, not from MoS_2, that is, E_F in WSe_2 is apart from VBM due to the *p*-doping reduction. For this *p*-doping reduction in WSe_2, two different origins can be considered. One is electron transfer from MoS_2; the other is that the top gate modulates p^+-WSe_2 as well as MoS_2.

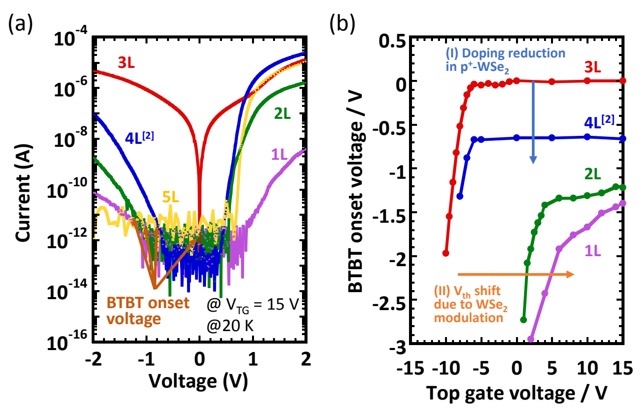

Fig. 4 (a) Diode properties and (b) BTBT onset voltage as functions of V_{TG} for p^+-WSe_2/1 - 5L MoS_2 devices.

Figure 5 illustrates band alignments controlled by above-mentioned two different physical origins. When p^+-WSe_2 is contacted with MoS_2, electron is transferred from MoS_2 to WSe_2 and E_F of WSe_2 uniformly increases because WSe_2 is doped by electron transfer to WO_x. Because the amount of transferred electron increases with increasing MoS_2 thickness, E_F of WSe_2 also changes by MoS_2 thickness and band alignment become type II for 4 and 5L-MoS_2 devices, which is shown by dotted blue line in **Fig. 5**. The band alignment change due to this charge transfer can be seen as (I) in **Fig. 4(b)**. In this consideration, type III should be obtained for 1L and 2L. However, when MoS_2 thickness is become thin like 1L and 2L, WSe_2 is also expected to be modulated by the top gate. Therefore, by applying V_{TG}, E_F in WSe_2 as well as MoS_2 is modulated at the same time, resulting to the type II from type III by decreasing MoS_2 thickness, as shown by a dotted orange line in **Fig. 5** and (II) in **Fig. 4(b)**. Because of these two different origins for *p*-doping reduction in WSe_2, only 3L MoS_2 shows type III.

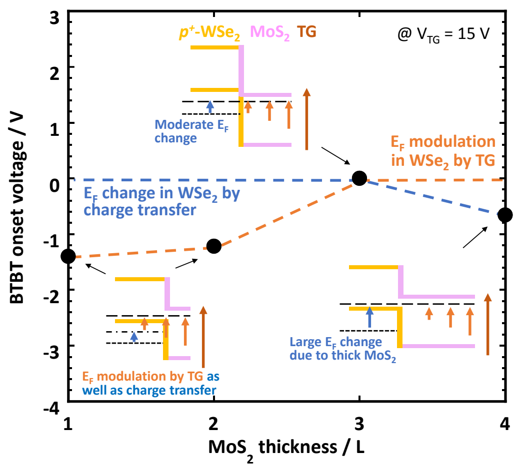

Fig. 5 V_{BTBT} as a function of MoS_2 thickness with the illustration of band alignment at V_{TG} = 15 V.

5. Conclusions

Through this study, it is revealed that band alignment of p^+-WSe_2/MoS_2 TFET is controlled by the two different physical origins, that is, E_F modulation in WSe_2 by V_{TG} and electron transfer from MoS_2. Since both origins depends on the MoS_2 channel thickness, the band alignment is quite sensitive to the MoS_2 thickness. This kind of drastic change with MoS_2 thickness happens because p^+-doping from WO_x is not high enough.

Acknowledgement: This research was partly supported by The Canon Foundation, the JSAP Core-to-Core Program, A. Advanced Research Networks, JSAP KAKENHI Grant Number JP19H00755, Japan. **References:** [1] A. M. Ionescu *et al.*, Nature 2011, **479**, 329. [2] J. He *et al.*, Adv. Electron. Mater. 2018, **4**, 1800207.